DOI: 10.19884/j.1672-5220.202409009

Automated Bionic Wig Weaving Process Design and Weaving Path Planning

LYU Hongzhan*, YOU Jia, LI Junjie, LU Licheng, SUN Zhihong
College of Mechanical Engineering, Donghua University, Shanghai 201620, China

Abstract: The traditional production of bionic wigs through manual weaving is a complex process characterized by high labor intensity, making automation challenging. To address this issue, an automated weaving process for bionic wigs is proposed and the design of an automated bionic wig weaving machine is presented based on an analysis of manual weaving principles and processes. Furthermore, according to the characteristics of the weaving machine and the distribution pattern of weaving nodes, the minimum weaving duration of a single hairnet is taken as the optimization goal, and a continuous weaving path planning for the weaving process of the mixed scheme is conducted. The weaving duration for various weaving paths are calculated and compared, and the results indicate that the duration of the S-shaped weaving path is always the shortest in different weaving regions. The designed automated weaving process and the weaving path planning provide a theoretical foundation and experimental data for achieving automated weaving of bionic wigs.

Keywords: bionic wig; weaving process; wig weaving machine; path planning
CLC number: TS9 **Document code**: A
Article ID: 1672-5220(2025)05-0550-08

Open Science Identity (OSID)

0 Introduction

China is a leading producer and exporter of wigs. In the year of 2022, global wig market has reached nearly 100 billion USD, with China accounting for 80% of worldwide exports[1]. Bionic wigs, primarily worn as aesthetic prostheses, are fabricated by manually weaving individual hair strands into lace hairnet[2], making the manual weaving process both time-consuming and labor-intensive. This time-consuming task has led to steadily rising labor costs. As the market demand for bionic wigs continues to surge, the need for automation in wig weaving is becoming increasingly urgent.

There has been extensive research on the automated wig weaving machines. It is disclosed in Ref. [3] that there is a motor-driven crochet in the experimental device to move hair. The principle is simple, but the device is large and exhibits low automation, and the continuity and precision of weaving cannot be guaranteed. Hiroshi[4] proposed an automated hair-transplant machine that utilized a vacuum generator to adhere artificial hair strands to the base of a hairnet. The hair strands were woven onto the hairnet by the up-and-down movement of a specialized crochet hook. However, due to its limited adsorption capabilities, the machine could only use artificial hair strands as raw materials in the weaving process. Kuang et al.[5] designed a wig weaving machine that employed a double cam mechanism to plan the crochet trajectory, and the weaving path of the machine was designed by adjusting the hairnet position with a two-dimensional numerical control table. However, the design remains semi-automatic, and manual adjustments and coordination are needed. Mitsuhiro et al.[6] introduced a manipulator with dual clamping mechanisms in the wig weaving. However, the absence of continuous path planning and the uncontrolled distribution of loose hair strands prevent the continuous weaving.

With the research on automated wig weaving machines, the wig weaving process has undergone continuous improvement and development. Lin[7] proposed a three-layer hairnet wig-making process, which involved weaving on two layers of the interlaced hairnet and then sewing them together at the bottom. Although this three-layer hairnet is sturdy, its breathability is very poor, and its unique structure is difficult to manufacture. Tao et al.[8] enhanced the traditional weaving process by adding elastic ropes to the folded ends of the hair strands, increasing the firmness of the hair knots. However, the steps are complicated and it is difficult for automation. Sun et al.[9] introduced a new wig weaving process suitable for automated weaving machines, utilizing a latch needle to complete the knotting action and produce double knots. This method is more suitable for automated weaving machines.

In summary, the concept of automated weaving machine for bionic wigs is still at the patent level, and there is currently no wig weaving device that can achieve automation in wig weaving. In this paper, the manual bionic wig weaving process is analyzed to enhance the

Received date: 2024-09-27
Foundation item: Yuzhou Olandi Arts & Crafts Co., Ltd., Project of Development and Research of Wig Planting Equipment, China (No. HX103210723)
* Correspondence should be addressed to LYU Hongzhan, email: lvhz@dhu.edu.cn
Citation: LYU H Z, YOU J, LI J J, et al. Automated bionic wig weaving process design and weaving path planning[J]. *Journal of Donghua University (English Edition)*, 2025, 42(5): 550-557.

design of an automated bionic wig weaving process based on existing manual wig weaving machines. Additionally, path planning during the weaving process is designed for the weaving machine.

1 Manual Bionic Wig Weaving Process

The manual bionic wig weaving consists of three key elements: a crochet, a hairnet and hair strands. The crochet is a specialized manual weaving tool with a barb on the front of the crochet. The hairnet is made of polyester lace and is composed of interwoven meshes with a height of 0.8 mm. The polyester lace material not only ensures adequate tension and elasticity but also possesses a degree of toughness which aids in crocheting and enhances the wig's durability[10]. Most ordinary wigs on the market are made from synthetic fibers[11] on the consideration of costs. However, the strength and texture of wigs made from these fibers are subpar[12], and their shaggy appearance significantly differs from that of human hair. Consequently, human hair is selected as a raw material for bionic wigs to achieve a more realistic effect. Combining the above three key elements, the final bionic wig product maintains a high degree of consistency with the human hair growth in terms of shape, smoothness and imitation.

In manual weaving, the worker coils the hair into a circle with one hand and operates the crochet with the other. Then the worker continuously twists the wrist to adjust the position of the crochet, and weaves the hair strands into knots along the common edge of the hairnet meshes. The double knot weaving process[13] is utilized in manual weaving, which employs the reverse half-buckle method to create double knots. The manual double knot weaving process is illustrated in Fig. 1.

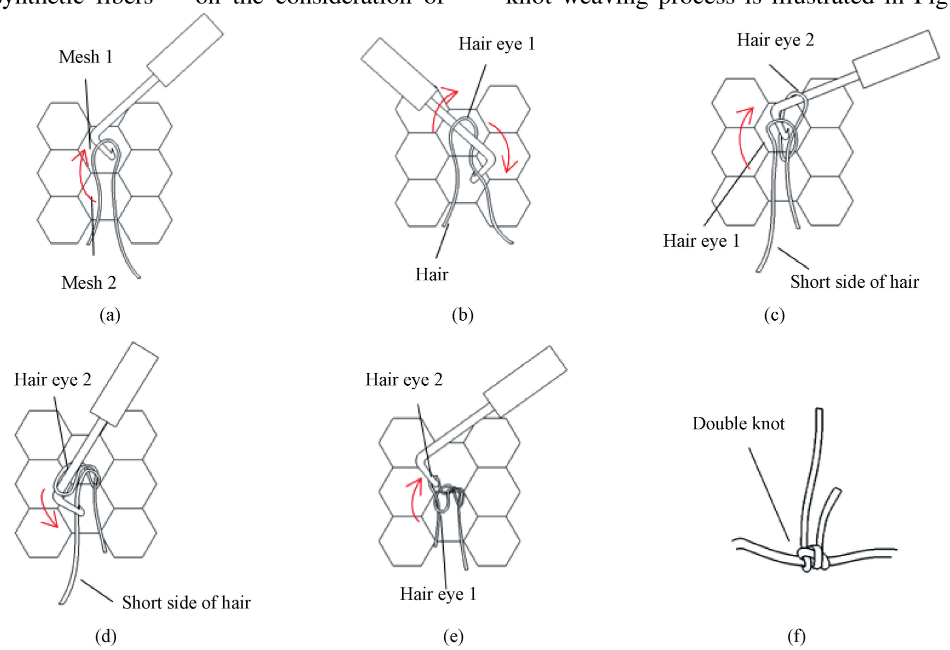

Fig. 1 Double knot weaving process: (a) crochet first feed; (b) hair eye 1 formation and crochet second feed; (c) hair eye 2 formation; (d) crochet third feed; (e) hook through hair eye 2; (f) double knot formation

2 Automated Bionic Wig Weaving Principle and Process Design

2.1 Automated bionic wig weaving machine and principle

To achieve the automation of the weaving process, an automated bionic wig weaving machine[14] is designed, as illustrated in Fig. 2. The weaving machine is primarily divided into three devices: the crochet drive device[15], the hairnet transmission device[16] and the hair conveying device[17]. These three devices correspond to the three essential elements of manual weaving: the crochet, the hairnet and the hair strands. During the weaving process, the crochet weaving action, continuous hairnet conveying and hair feeding are performed, respectively.

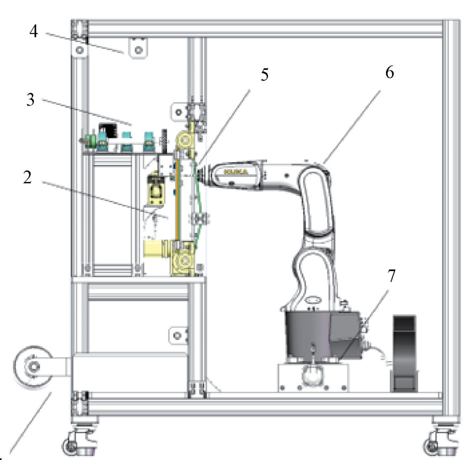

1—winder; 2—hairnet transmission device; 3—hair conveying device; 4—roller; 5—latch needle; 6—corobot; 7—ground rail.

Fig. 2 Model of automated bionic wig weaving machine

Figure 3 is the schematic diagram of the automated bionic wig weaving machine. According to the requirements of manual weaving, improvements are made to address the complex weaving actions involved in the crochet. The hairnet is repositioned vertically, and the original barbed crochet is replaced with a latch needle, which is now placed at the front of the hairnet. The hair conveying device organizes the hair strands into a uniform and evenly distributed curtain which is positioned at the rear end of the hairnet. When the weaving machine is in operation, the corobot controls the latch needle to execute a series of knotting actions, and the process is modularized. The ground rail is located at the bottom of the corobot, and it drives the corobot to move horizontally to complete the horizontal weaving of the hairnet. The hairnet transmission device longitudinally moves the hairnet to complete the longitudinal weaving.

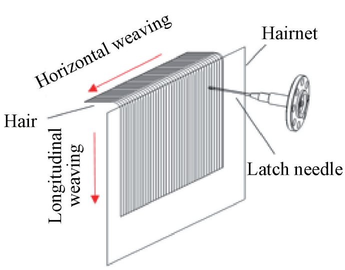

Fig. 3 Schematic diagram of automated bionic wig weaving machine

2.2 Automated bionic wig weaving process design

In order to ensure the efficiency and quality of automated weaving, the automated weaving process is designed based on the double knot weaving process. The relative movement of the crochet and hairnet in the weaving process of a double knot is shown in Fig. 4. The movement of the crochet in the automated process is divided into nine decomposition actions to achieve the automated weaving of a double knot.

The weaving of a double knot involves two adjacent meshes, namely mesh 1 and mesh 2. The entire automated bionic wig weaving process can be divided into four phases. In the first phase, the crochet is inserted diagonally through mesh 1 to pick up the hair strands and pull them out, as shown in Figs. 4(a)–4(c). The hair strands create a loop at the common edge of the two meshes, referred to as hair eye 1. In the second phase, the crochet hooks the long edge of the hair through mesh 2, forming a loop with hair eye 1, which is designated as hair eye 2, as shown in Figs. 4(d)–4(e). In the third phase, the crochet hooks the short edge of the hair completely out of mesh 2 from hair eye 2, as shown in Figs. 4(f)–4(g). In the fourth phase, the long edge of the hair is fully extracted, resulting in a double knot, as shown in Figs. 4(h)–4(i). Compared with the manual weaving process, the automated weaving process only alters the initial layout of key elements. In the step of forming a double knot, both the two processes involve two adjacent meshes, and the composition of hair eye 1 and hair eye 2 formed during weaving is the same. Therefore, the double knot produced in the automated weaving process is consistent in quality with that produced in the manual weaving process.

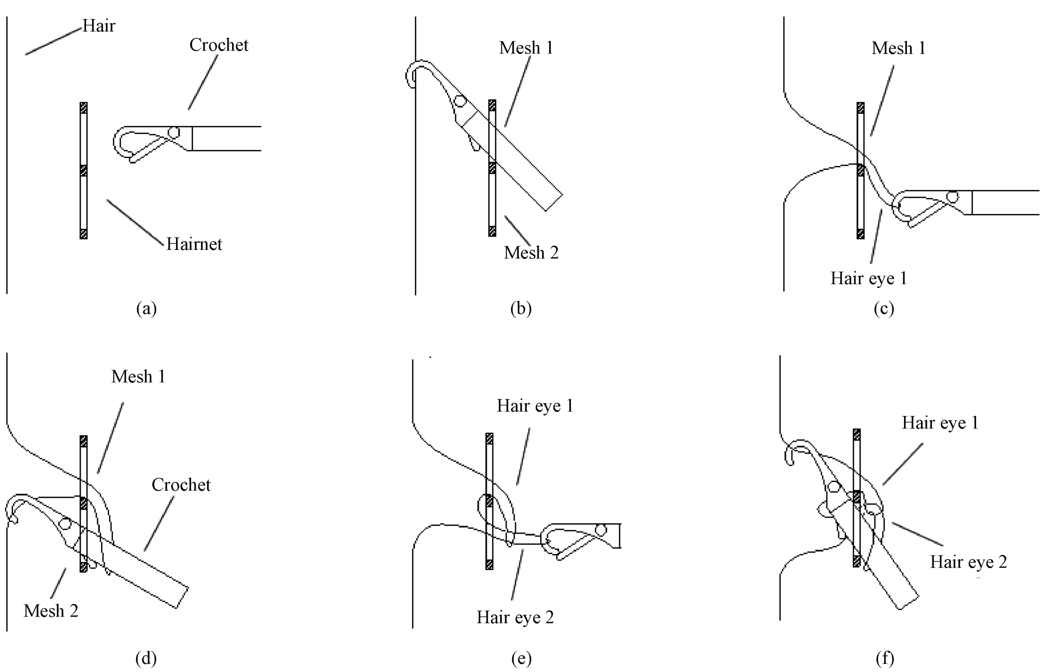

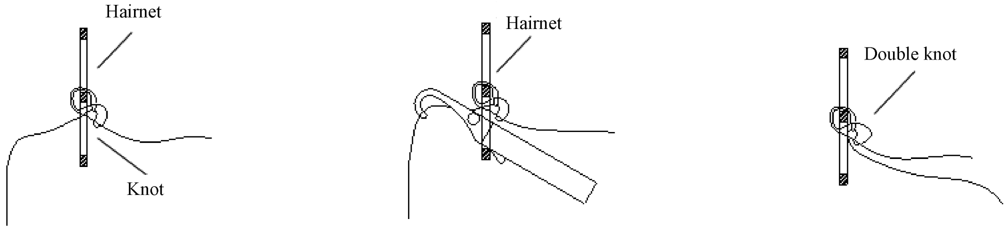

(g) (h) (i)

Fig. 4 Automated bionic wig weaving process: (a) initial placement; (b) crochet first feed; (c) hair eye 1 formation; (d) crochet second feed; (e) hair eye 2 formation; (f) crochet third feed; (g) knot formation; (h) crochet fourth feed; (i) double knot formation

3 Automated Bionic Wig Weaving Path Planning

To achieve continuous weaving of the entire hairnet, it is essential to plan the weaving path. The hairnet is staggered by a grid of regular hexagons, and the weaving nodes are located along the common sides of the hexagons. The distance between adjacent transverse weaving nodes is 1.386 mm, while the vertical distance between two longitudinal weaving nodes is 0.800 mm. All the weaving nodes on the hairnet collectively form a single area shaped like a hairnet, as illustrated in Fig. 5. This area can be divided into two distinct regions, namely the rectangular region and the semicircular region.

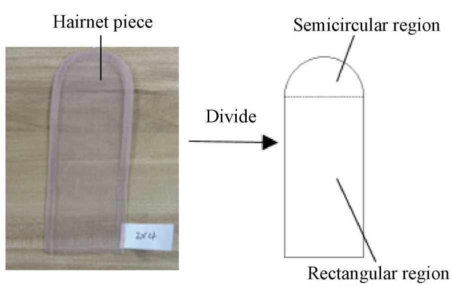

Fig. 5 Region division of hairnet piece

A shorter weaving path can reduce weaving duration and correspondingly increase the weaving efficiency. During the weaving process of a hairnet, the rectangular region and the semicircular region need to be completed in sequence. Therefore, the shortest total weaving duration of a single hairnet can be expressed as

$$\min T_W = \min T_R + \min T_S, \tag{1}$$

where T_W represents the total weaving duration of a single hairnet; T_R denotes the total weaving duration of a rectangular region; T_S indicates the total weaving duration of a semicircular region.

3.1 Weaving path in rectangular region

The distribution of weaving nodes in the rectangular region is shown in Fig. 6. All the odd rows contain the same number of weaving nodes. All the even rows contain the same number of weaving nodes. Due to the alternating grid distribution, even rows have one fewer weaving node than odd rows. Suppose the total number of rows in the rectangular region is n, where n is even, and the total number of weaving nodes in the first row is m, where m is odd. Then the total number of weaving nodes in the second row will be $m-1$, and the number of weaving nodes in the subsequent rows is cycled in turn.

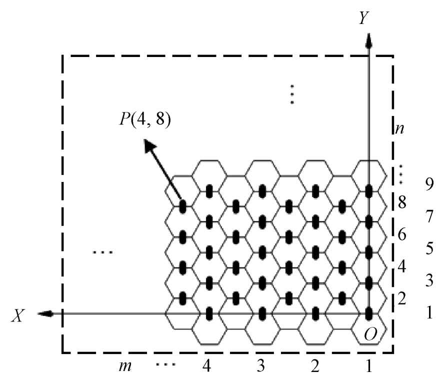

Fig. 6 Distribution of weaving nodes in rectangular region

Take the lower right corner of the rectangular region as the weaving origin, the positive direction of the X axis extends to the left, while the positive direction of the Y axis extends upward. Any weaving node on the hairnet can be represented as $P(m, n)$. For example, the weaving node marked in Fig. 6 is denoted as $P(4, 8)$. Then the shortest total weaving duration in the rectangular region is

$$\min T_R = \min t_1 + \min t_2, \tag{2}$$

where t_1 represents the total knotting duration of all weaving nodes; t_2 represents the total movement duration including the total horizontal movement time and the total longitudinal movement time. The entire weaving of the rectangular region can be regarded as a set from a weaving node P_i to the next weaving node P_j. Let the coordinates of P_i be denoted as $P(m_i, n_i)$, and the coordinates of P_j be denoted as $P(m_j, n_j)$. Then the formula can be obtained

$$t_1 = N_W t_W, \tag{3}$$

where N_W is the number of all weaving nodes in the rectangular region; t_W is the weaving duration of one node. Since P_i and P_j are weaving nodes within the rectangular region, it can be obtained that

$$\forall i \in \{1, 2, \cdots, N_w - 1\}, \quad j \in \{2, 3, \cdots, N_w\}, j - i = 1, \tag{4}$$

$$t_2 = \sum_{i=1}^{N_w-1} \sum_{j=2}^{N_w} x_{ij} t_H + \sum_{i=1}^{N_w-1} \sum_{j=2}^{N_w} y_{ij} t_L, \tag{5}$$

$$x_{ij} = \begin{cases} 2, \text{ when } |n_i - n_j| = 0, \\ 1, \text{ when } |n_i - n_j| = 1, \\ 0, \text{ others}, \end{cases} \tag{6}$$

$$y_{ij} = |n_i - n_j|, \tag{7}$$

where t_H is the duration required to move half the spacing between two horizontally adjacent nodes; t_L is the duration required to move the full spacing between two longitudinally adjacent nodes; x_{ij} is the coefficient of the horizontal distance from P_i to P_j; y_{ij} is the coefficient of the longitudinal distance from P_i to P_j.

The entire rectangular region can be viewed as a loop formed by the first two rows of weaving nodes. Therefore, as long as the fastest weaving path for the first two rows is determined, the optimal weaving path for the entire rectangular region can be established. The first two rows of weaving nodes within the rectangular region are designated as the object, and based on their distribution, two primary weaving paths have been identified as shown in Fig. 7: the S-shaped weaving path and the folding weaving path. In the S-shaped weaving path, the weaving path first begins from $P(1, 1)$ to the left until reaching $P(m, 1)$; then, the weaving path in the second row starts from $P(m-1, 2)$ to the right until reaching $P(1, 2)$. While in the folding weaving path, the nearest node is selected as the next weaving node. The weaving path starts from $P(1, 1)$ to $P(1, 2)$, and then to $P(2, 1)$, and proceeds until reaching the final node $P(m, 1)$; after the two rows of weaving are completed, the path transitions to $P(m, 3)$ to initiate a new round of two-row cyclic weaving.

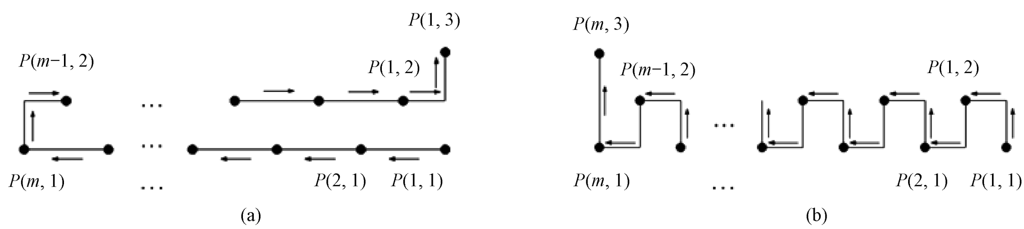

Fig. 7 Two weaving paths in rectangular region: (a) S-shaped weaving path; (b) folding weaving path

The weaving duration comparison of the above two weaving paths is shown in Table 1. The knotting duration is related to the number of all weaving nodes, so it is the same for the two weaving paths. Thus, the movement duration in the moving process is compared. Since the speed of the horizontal and longitudinal movements is the same, the comparison of the movement duration can be converted into a comparison of the distance as shown in Table 1. As m is a large positive integer, the corresponding distance of the S-shaped weaving path is shorter than that of the folding weaving path. The weaving duration of the S-shaped weaving path is shorter and the efficiency is higher. As a result, the S-shaped weaving path is selected in the rectangular region.

Table 1 Weaving duration comparison of two weaving paths in rectangular region

Weaving path	Knotting duration	Horizontal movement duration	Longitudinal movement duration	Corresponding distance
S-shaped weaving	$(2m - 1)t_W$	$4(m - 1)t_H$	$2t_L$	$2.772m - 0.907$
Folding weaving	$(2m - 1)t_W$	$2(m - 1)t_H$	$2mt_L$	$2.986m - 1.386$

3.2 Weaving path in semicircular region

The distribution of weaving nodes in the semicircular region is illustrated in Fig. 8. The alternating weaving nodes create the shape of the semicircle. As stated in subsection 3.1, row n of the rectangular region contains $m-1$ weaving nodes. Therefore, the first row of the semicircular region contains m weaving nodes. The semicircular region consists of a total of $(m-1)/2$ rows. With the center of the semicircular region as the boundary, the X axis and Y axis are established to ensure that all nodes are symmetrically distributed on both sides of the Y axis.

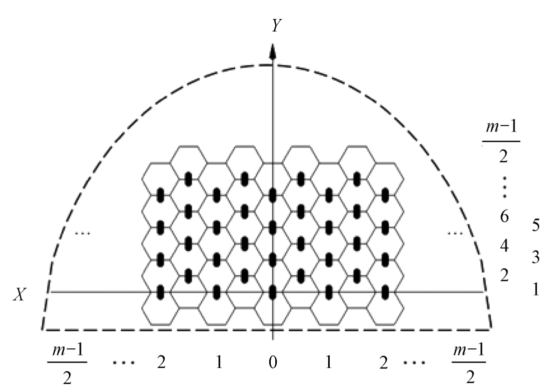

Fig. 8 Distribution of weaving nodes in semicircular region

Starting from the first row and moving upward, the number of weaving nodes in the odd-numbered rows decreases in an arithmetic sequence with a common difference denoted as k. Additionally, the difference in the number of weaving nodes between each odd-numbered row and the even-numbered row above it is a fixed value, denoted as a, where a is an odd number. In the semicircular region, the weaving order remains from the bottom up, and the shortest weaving duration of the semicircular weaving path is

$$\min T_S = t_1 + t_2. \quad (8)$$

Based on the distribution of weaving nodes and the weaving requirements, there are two types of weaving paths in the semicircular region as shown in Fig. 9: the S-shaped weaving path and the mixed weaving path.

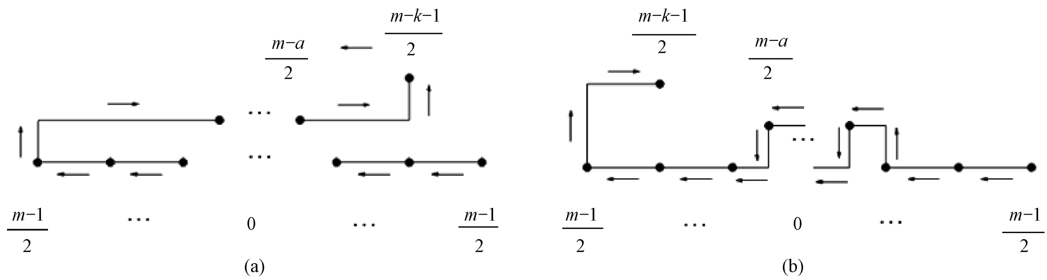

Fig. 9 Two weaving paths in semicircular region: (a) S-shaped weaving path; (b) mixed weaving path

In the S-shaped weaving path, the weaving path begins at the rightmost end and proceeds sequentially through the first row of m weaving nodes. The weaving path then moves to the outermost node in the second row and continues from left to right. The mixed weaving path is a combination of S-shaped weaving and folding weaving. The second row contains a fewer weaving nodes than the first row, resulting in no weaving nodes above the outermost nodes of the first row. Consequently, the outer section employs S-shaped weaving, while the middle section utilizes folding weaving. After completing the weaving of the two rows, the weaving path stops at the leftmost node of the first row. In the rectangular region, after completing the first two rows, the S-shaped weaving path must transition from the rightmost node in the second row to the rightmost node in the third row to continue with the next two rows. In contrast, the mixed weaving path requires a movement from the leftmost node in the first row to the leftmost node in the third row. Both weaving paths necessitate additional movement along a specific route. Consequently, Eq. (5) has been revised to incorporate a compensation distance for this movement.

$$t_2 = \sum_{i=1}^{N_w-1}\sum_{j=2}^{N_w} x_{ij}t_H + \sum_{i=1}^{N_w-1}\sum_{j=2}^{N_w} y_{ij}t_L + \sum_{p=1}^{(m-1)/2} e_p t_H + \sum_{q=1}^{(m-1)/2} e_q t_L, \quad (9)$$

$$e_q = \begin{cases} |n_i - n_j|, \text{ when } |n_i - n_j| \in \{0,1\}, \\ 0, \text{ others}, \end{cases} \quad (10)$$

$$e_p = \begin{cases} k, \text{ when } |n_i - n_j| = 2, \\ a - k, \text{ others}, \end{cases} \quad (11)$$

where e_q is the compensation factor for the additional longitudinal movement; e_p is the compensation factor for the additional horizontal movement. Since the total number of weaving nodes is the same, the knotting duration is also the same. To compare the movement duration of the two weaving paths, the specific durations are converted into their corresponding distances as shown in Table 2.

Table 2 Weaving duration comparison of two weaving paths in semicircular region

Weaving path	Horizontal movement duration	Longitudinal movement duration	Compensation duration	Corresponding distance
S-shaped weaving	$(4m-4-a)t_H$	t_L	$t_L + (a-k)t_H$	$2.772m-0.693k-1.172$
Mixed weaving	$2(m-1)t_H$	$2(m-a)t_L$	$2t_L + kt_H$	$2.986m+0.693k-1.6a+0.214$

Subtract the corresponding distance of the mixed weaving path from that of the S-shaped weaving path to obtain their difference Δf

$$\Delta f = 0.214m + 1.386k - 1.6a + 1.386. \quad (12)$$

According to the specific dimensions of the hairnet, m is a number larger than 41. This indicates that m is a large positive integer. Additionally, in order to ensure the number of rows in the hairnet, a and k serving as decreasing factor parameters, should be small positive integers. Compared to the numbers and parameters appearing in Eq. (12), m is obviously much larger than them. Therefore, considering the actual conditions of hairnet weaving, the condition $\Delta f > 0$ always holds. This means that the weaving duration for the mixed weaving path is longer than that for the S-shaped weaving path.

Consequently, in order to maintain the weaving efficiency, the S-shaped weaving path is also selected in the semicircular region.

3.3 Experimental verification of weaving path

To verify the feasibility of the proposed shortest weaving path, experiments are conducted by using the designed automated bionic wig weaving machine, as illustrated in Fig. 10. A standard-sized hairnet (5.08 cm × 10.16 cm) is selected as the weaving target, and the movement duration across the area of a single hairnet is recorded. According to the designed weaving path, the S-shaped weaving and folding weaving paths are employed in the rectangular region, while the S-shaped weaving and mixed weaving paths are utilized in the semicircular region. Three groups of the movement duration for different weaving paths in both regions are measured in the experiment, as shown in Table 3.

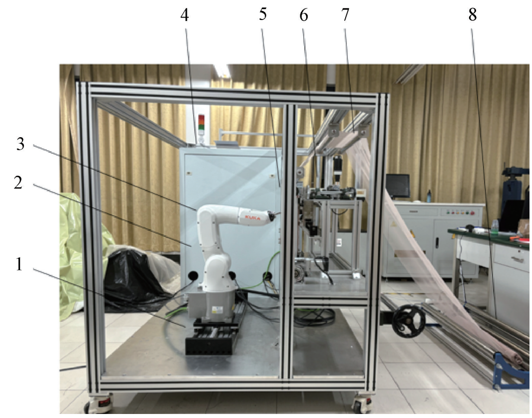

1—ground rail; 2—crochet drive device; 3—corobot; 4—electrical cabinet; 5—hairnet transmission device; 6—hair conveying device; 7—hairnet roll; 8—uncoiler.

Fig. 10 Automated bionic wig weaving machine

Table 3 Movement duration of different weaving paths in each region

Region and weaving path	The first group of movement duration/s	The second group of movement duration/s	The third group of movement duration/s
S-shaped weaving path in rectangular region	6 649.6	6 651.8	6 652.1
Folding weaving path in rectangular region	7 202.5	7 203.6	7 204.5
S-shaped weaving path in semicircular region	704.6	703.5	703.9
Mixed weaving path in semicircular region	774.3	773.6	772.8

In the rectangular region, the movement duration of the S-shaped weaving path saves about 550 s, and the efficiency increases by about 7.7% compared with that of the folding weaving path. In the semicircular region, the movement duration of the S-shaped weaving path saves about 70 s and the efficiency increases by about 9.0% compared with that of the mixed weaving path. The weaving path planning proposed above is accurate, and the S-shaped weaving path is the most efficient.

4 Conclusions

A design for an automated bionic wig weaving process is presented and an automated bionic wig weaving machine is developed along with the conduction of weaving path planning. The main conclusions are as follows.

1) The automated bionic wig weaving process designed in this paper changes the layout of the three elements of manual weaving. The designed automated bionic wig weaving machine can realize horizontal and longitudinal weaving, making the automated continuous weaving of bionic wigs possible.

2) Taking the shortest weaving duration of a single hairnet as the objective function, the theoretical calculations and specific experiments are conducted respectively on the weaving duration of each path in the rectangular region and the semicircular region. In the rectangular region, the efficiency of the S-shaped weaving path increases by 7.7% compared with that of the folding weaving path; in the semicircular region, the efficiency of the S-shaped weaving path increases by 9.0% compared with that of the mixed weaving path.

References

[1] ZHANG Y. Rural revitalization industry needs such "unexpected" [N]. *Haidong Daily*, 2022-03-26 (001). (in Chinese)

[2] LIU G M. Xuchang wig industry export: leverage advantages to produce high-quality products [N]. *China Trade News*, 2022-07-07 (007). (in Chinese)

[3] MAZEKO ENTERPRISES, INC. Apparatus for implanting hair in manikins, dolls, and the like: US19490124305[P]. 1954-02-02.

[4] HIROSHI H. Automated hair-transplanting machine for making and method of transplanting hair: JP20000129955 [P]. 2001-10-31. (in Japanese)

[5] KUANG Z W, LI W G, KONG Z H, et al. Semi-automatic machine models in hair weaving [J]. *Mechanical Engineer*, 2007(9): 129-131. (in Chinese)

[6] MITSUHIRO M, SHINICHI K, KOUJI M, et al. Hair implant device and method for manufacturing wig using hair implant device: JP2021043944[P]. 2022-06-09. (in Japanese)

[7] LIN C H. A production process for wigs that uses a three-layer mesh: CN107028263A[P]. 2017-

08-11. (in Chinese)
[8] TAO L, JIN Y C. A weaving technique for wigs: CN105708021B [P]. 2017-09-29. (in Chinese)
[9] SUN Z H, LYU H Z, ZHANG B M, et al. A method for knotting hair transplant wigs: CN114224004A[P]. 2022-03-25. (in Chinese)
[10] QIU H, XIE N W, ZHANG W, et al. Preparation of PET/PU elastic nonwoven material [J]. *China Synthetic Fiber Industry*, 2017, 40(2): 17-20. (in Chinese)
[11] PEI Y H, YU H. Discussion on the application status and problems of wig materials [J]. *Synthetic Fiber in China*, 2022, 51(12): 28-31. (in Chinese)
[12] CHENG H M. Process technology design of imitated synthetic hair fiber [D]. Shanghai: Donghua University, 2014. (in Chinese)
[13] CAI C R. Research on the process of wig production and the key mechanisms of wig production equipment [D]. Shanghai: Donghua University, 2023. (in Chinese)
[14] LYU H Z, SUN Z H, ZHANG B M, et al. A fully automated wig planting machine: CN202210932166.1 [P]. 2022-11-11. (in Chinese)
[15] LYU H Z, SUN Z H, ZHANG B M, et al. A crochet drive device used in wig weaving machine: CN202210932174.6[P]. 2022-11-01. (in Chinese)
[16] LYU H Z, SUN Z H, ZHANG B M, et al. A control device for hairnet used in wig weaving machine: CN202210931474.2[P]. 2022-11-11. (in Chinese)
[17] SUN Z H, LYU H Z, WU J M, et al. A hair strand clamping and feeding device for wig weaving machine: CN202210932172.7 [P]. 2024-07-30. (in Chinese)

仿生假发自动化织造工艺设计与织造路径规划

吕宏展*，尤　佳，李俊杰，陆李承，孙志宏
东华大学 机械工程学院，上海 201620

摘　要：传统的仿生假发生产由工人手工织造完成，织造工艺过程复杂，劳动强度大，很难实现自动化。针对该问题，在手工织造原理与工艺分析的基础上，本文提出了自动化织造工艺和自动假发织造机的设计。根据该织造机的特点和织造结点分布规律，以单张发网的总织造时长最短为优化目标，对混合方案的织造工艺进行了连续织造路径规划。分别计算并对比不同织造路径的织造时长，结果表明 S 型路径的织造时长最短。该自动化织造工艺设计与织造路径规划方法为仿生假发自动化织造的实现提供了理论依据和试验数据。

关键词：仿生假发；织造工艺；假发织造机；路径规划